Equivalent Circuit Models for Three-Dimensional Multiconductor Systems

ALBERT E. RUEHLI, MEMBER, IEEE

Abstract—**Multiconductor or multiwire arrangements find many applications in electronic systems. Examples are interconnections between digital circuits or integrated microwave circuits. Equivalent circuit models are derived here from an integral equation to establish an electrical description of the physical geometry. The models, which are appropriately called partial element equivalent circuits (PEEC), are general in that they include losses. Models of different complexity can be constructed to suit the application at hand.**

I. Introduction

MULTICONDUCTOR or multiwire arrangements find many applications in electronic systems, e.g., the intercommunications between digital logic circuits [1] or microwave integrated circuits [2]. Several methods are available today for the analysis of a set of long parallel wires close to a common conducting plane [3]–[5]. Two-dimensional approximations are, however, not applicable to an important class of three-dimensional conductor arrangements. These geometries consist of conductors that may be highly intercoupled because of the absence or remoteness of a common ground plane. Examples of three-dimensional geometries are integrated circuit packages and wires or conductors located on dielectric layers with remote ground planes. These geometries may be viewed as "consisting of discontinuities" from a transmission line point of view and are not easily amenable to analysis. However, additional electrical design flexibility is obtained above two-dimensional striplines for many applications due to the multitude of relative conductor locations possible.

The purpose of this paper is to present a theory for an approximate computer modeling approach for three-dimensional geometries that is appropriately called partial element equivalent circuit (PEEC) analysis. The PEEC method is based on an integral equation description of the geometry that is interpreted in terms of circuit elements. The circuit elements, viz., the partial inductances and partial capacitances, can be found from computer solutions, as has been shown previously [6]–[9]. A general-purpose network analysis program [10]–[12] is then used to obtain voltages and currents in both the time domain and the frequency domain. Time domain results are given here and elsewhere [13] since they encompass a wide frequency spectrum.

The formulation presented here affects three seemingly different subject areas. First, it provides a more comprehensive interpretation of the relations between circuit theory and field theory [14]. Second, it may be considered as an extension of an integral equation solution for inductance computations [15] in that it includes capacitance. Third, it relates to multiwire antennas [16], which corresponds to the formulation below if retardation times are included.

A basic integral equation approach is discussed in Section II, while an interpretation in terms of inductances is considered in Section III. The portion that relates to capacitance is the subject of Section IV, and in Section V the relation to retardation times is discussed. In Section VI circuit interpretations are considered, while in Section VII an example is given and further approximations are discussed.

II. Integral Equation Formulation

The unknowns in a multiconductor or multiwire system are the charges on the surfaces and the current densities within the conductors. An integral equation solution is appropriate for problems with large free-space regions since a differential equation formulation would require that all regions including the free space be described by nodes.

The approximate integral equation solution pursued here is based on the summation of all sources of electric fields within a conductor [14], or $\bar{J}/\sigma = \bar{E}_0 - \partial\bar{A}/\partial t - \nabla\Phi$. Here, $\bar{J}$ is the current density in the conductor of conductivity σ, and $\bar{A}$ and Φ are the vector and scalar potentials, respectively.

$$\bar{E}_0(\bar{r},t) = \frac{\bar{J}(\bar{r},t)}{\sigma} + \frac{\partial\bar{A}(\bar{r},t)}{\partial t} + \nabla\Phi(\bar{r},t) \tag{1}$$

where $\bar{r}$ is the vector from the origin. The vector potential $\bar{A}$ for K conductors is

$$\bar{A}(\bar{r},t) = \sum_{k=1}^{K} \frac{\mu}{4\pi} \int_{v_k} \tilde{K}(\bar{r},\bar{r}')\bar{J}(\bar{r}',t')\, dv' \tag{2}$$

where the retarded time is given by

$$t' = t - \frac{|\bar{r} - \bar{r}'|}{c} (\epsilon_r\mu_r)^{1/2} \tag{3}$$

Manuscript received June 25, 1973; revised September 28, 1973.
The author is with the Circuit and Computer Design Automation Group, IBM Thomas J. Watson Research Center, Yorktown Heights, N. Y. 10598.

for uniform regions with properties ϵ_r, μ_r, where c represents the speed of light. The function $\tilde{K}$ is defined by

$$\tilde{K}(\bar{r},\bar{r}') \triangleq \frac{1}{|\bar{r}-\bar{r}'|}. \tag{4}$$

Similarly, the scalar potential Φ is

$$\Phi(\bar{r},t) = \sum_{k=1}^{K} \frac{1}{4\pi\epsilon} \int_{v_k} \tilde{K}(\bar{r},\bar{r}')q(\bar{r}',t')\, dv'. \tag{5}$$

Inserting (2) and (5) into (1) leads to

$$\bar{E}_0(\bar{r},t) = \frac{\bar{J}(\bar{r},t)}{\sigma} + \sum_{k=1}^{K} \frac{\partial}{\partial t}\left[\frac{\mu}{4\pi}\int_{v_k} \tilde{K}(\bar{r},\bar{r}')\bar{J}(\bar{r}',t')\, dv'\right] + \sum_{k=1}^{K} \nabla\left[\frac{1}{4\pi\epsilon}\int_{v_k} \tilde{K}(\bar{r},\bar{r}')q(\bar{r}',t')\, dv'\right]. \tag{6}$$

As a first step towards a PEEC representation, the unknown quantities are approximated as locally constant functions. The current density is represented in terms of orthogonal components, or $\bar{J} = J_x\hat{x} + J_y\hat{y} + J_z\hat{z}$, where the components are locally constant over cells to be chosen. A rectangular volume cell is defined by a pulse function [16] as $P_{\gamma nk} = 1$ on the γnkth volume cell and is 0 elsewhere. Here, $\gamma = x,y,z$ and nk represents the nth element on conductor k. The current density is then expanded as

$$J_{\gamma k}(t') = \sum_{n=1}^{N_{\gamma k}} P_{\gamma nk} J_{\gamma nk}(t_n) \tag{7}$$

where t_n is an approximation of t' and is given by

$$t_n \triangleq t - \frac{|\bar{r}-\bar{r}_n|}{c}(\epsilon_r\mu_r)^{1/2}. \tag{8}$$

The vector $\bar{r}_n$ extends to the center of the source volume cell, and $N_{\gamma k}$ is the total number of cells in the γ direction on conductor k. The expansion function (7) is inserted into the general equation (6) to yield

$$E_{0\gamma}(\bar{r},t) = \frac{J_\gamma(\bar{r},t)}{\sigma} + \sum_{k=1}^{K}\sum_{n=1}^{N_{\gamma k}} \frac{\mu}{4\pi}\left[\int_{v_{nk}} \tilde{K}(\bar{r},\bar{r}')\, dv'\right]\frac{\partial J_{\gamma nk}(t_n)}{\partial t} + \sum_{k=1}^{K} \frac{\partial}{\partial\gamma}\left[\frac{1}{4\pi\epsilon}\int_{v_k} \tilde{K}(\bar{r},\bar{r}')q(\bar{r}',t')\, dv'\right] \tag{9}$$

for $\gamma = x,y,z$.

Furthermore, the charge density is written as another expansion function of the same type. Since the free charge is restricted to the outside surfaces of all conductors, $q(\bar{r})$ is a surface layer charge density rather than a volume quantity. Hence, the expansion function for the charge density is

$$q_k(t_m) = \sum_{m=1}^{M_k} p_{mk} q_{mk}(t_m) \tag{10}$$

where M_k includes all surface cells charged with a locally constant charge density. The extent of the surface cell is defined as $p_{mk} = 1$ on the mth cell and is 0 elsewhere. An example is given for an appropriate choice of the cells, before this development is carried further. The number of network nodes specified within a conductor determines the size of the cells and, ultimately, the complexity of the networks. The number of nodes should not be exceedingly large for practical solutions. Fig. 1 shows a choice of cells for the most general case, a conductor with finite thickness for all three directions of current flow. The dividing lines are called inductive–resistive partitions and the choice of the cells at each node in uniquely given by the nodes. An appropriate division of the conductor surface into mutually exclusive uniformly charged cells is shown in Fig. 2. The dividing lines that disconnect the surface electrically are called capacitive partitions. The elements of the equivalent circuits are fully determined by these cells.

It is recognized that the applied field $\bar{E}_0$ is 0 for the circuit problem under consideration. A set of coupled equations is obtained next by integration of (9) separately over all volume cells into which the K conductors are divided. Integration over the lth cell in one of the conductors leads to

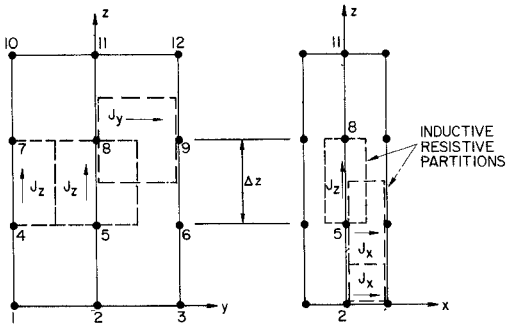

Fig. 1. Volume cells for currents in rectangular conductor.

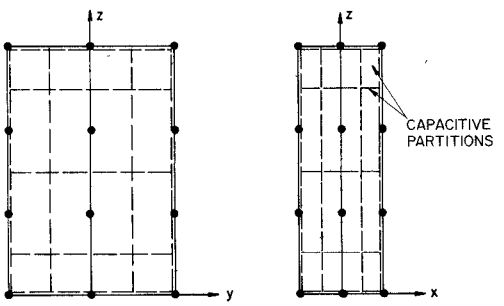

Fig. 2. Surface cells for capacitive partitions for rectangular conductors.

$$\frac{1}{\sigma}\int_{v_l} J_\gamma(\bar{r},t)\,dv_l + \sum_{k=1}^{K}\sum_{n=1}^{N_{\gamma k}}\frac{\mu}{4\pi}\left[\int_{v_l}\int_{v_{nk}}\tilde{K}(\bar{r},\bar{r}')\,dv'\,dv_l\right]\frac{\partial J_{\gamma nk}(t_n)}{\partial t} + \sum_{k=1}^{K}\frac{1}{4\pi\epsilon}\int_{v_l}\frac{\partial}{\partial\gamma}\left[\int_{Sk}\tilde{K}(\bar{r},\bar{r}')q(\bar{r}',t')\,ds'\right]dv_l = 0 \quad (11)$$

where $\gamma = x,y,z$ as previously, where the charge density is included as a surface quantity in (11). Next, (11) is divided by the cell cross section a_l perpendicular to the direction of current flow. The local approximations used here to find network elements are the same as are used in finite difference techniques. The first term on the left-hand side of (11) is then interpreted as the resistive voltage drop along the cell $v_r = R_{\gamma l}I_{\gamma l}$ and (11) is rewritten as $v_r + v_L + v_c = 0$.

III. Inductance Term

The second term on the left-hand side is rewritten in terms of the total current through the cell as

$$v_L = \sum_{k=1}^{K}\sum_{n=1}^{M_{\gamma k}}\left[\frac{\mu}{4\pi}\frac{1}{a_l a_{\gamma nk}}\int_{v_l}\int_{v_{nk}}\tilde{K}(\bar{r},\bar{r}')\,dv'\,dv_l\right]\frac{\partial I_{\gamma nk}(t_n)}{\partial t}. \quad (12)$$

If the kernel (4) is inserted into (12), the term in brackets is recognized to be in the form of partial inductances [6], with the sums representing the coupling among them:

$$v_L = \sum_{k=1}^{K}\sum_{n=1}^{N_{\gamma k}} Lp_{l,\gamma nk}\frac{d}{dt}[I_{\gamma nk}(t_{nk})]. \quad (13)$$

Again, the inductances of straight conductor segments corresponding to the cells are called partial inductances L_{pij} to avoid confusion with the loop inductances L_{ij}. The currents $I_{\gamma nk}$ are for most practical systems instantaneous in that $t_n = t$ in (8), due to physical smallness. For widely spaced segments in uniform regions, retarded partial inductances can be defined since the retardation depends on the physical distance.

IV. Capacitive Term

It is next shown that the last term in (11) corresponds to capacitive coupling. The inside integral is defined as $F(\gamma) \triangleq \int_{s_{mk}} \tilde{K}q\,ds'$ over the local surface cells defined in (10). Then the integral in the γ coordinate is approximated as

$$\int_{v_l}\frac{\partial}{\partial\gamma}F(\gamma)\,dv_l \doteq a_l\left[F\left(\gamma+\frac{\Delta\gamma}{2}\right) - F\left(\gamma-\frac{\Delta\gamma}{2}\right)\right]. \quad (14)$$

This shows that the capacitive cells in Fig. 2 are shifted from the cells in Fig. 1 by half the size of a cell. If the above results are applied to (11) and use is made of (10), a circuit-type equation results, or

$$v_c = \sum_{k=1}^{K}\sum_{m=1}^{M_k}\left[q_{mk}(t_{mk})\frac{1}{4\pi\epsilon}\int_{S_{mk}}\tilde{K}(\bar{r}_l^+,\bar{r}')\,ds' - q_{mk}(t_{mk})\frac{1}{4\pi\epsilon}\int_{S_{mk}}\tilde{K}(\bar{r}_l^-,\bar{r}')\,ds'\right]. \quad (15)$$

The vector associated with the positive end of the lth cell is designated with a + sign while the negative lead is indicated with a − sign. The retarded time refers to the center of the volume cell, in the same way as for the partial inductances. The kernel for the integrals in (15) is rewritten as a Green's function $G = K/4\pi\epsilon$. Then (15) is

$$v_c = \sum_{k=1}^{K}\sum_{m=1}^{M_k} q_{mk}(t_{mk})\left[\int_{S_{mk}} G(\bar{r}_l^+,\bar{r}')\,ds' - \int_{S_{mk}} G(\bar{r}_l^-,\bar{r}')\,ds'\right]. \quad (16)$$

With the total charge on the mkth cell given by $Q_{mk} = q_{mk}a_{mk}$, the terms in (16) can easily be interpreted as

$$v_c = \sum_{k=1}^{K}\sum_{m=1}^{M_k} Q_{mk}(t_{mk})[pp_{i(mk)}{}^+ - pp_{i(mk)}{}^-] \quad (17a)$$

where in general

$$pp_{ij} = \frac{1}{a_j}\int_{S_j} G(\bar{r}_i,\bar{r}')\,ds'. \quad (17b)$$

Equation (17) is clearly in the form of partial coefficients of potential (7), which is essentially the same as the coefficients of potential except that partial surfaces of a conductor are involved. Equation (17a) represents the voltage differences $V_{ij} = \Phi_i - \Phi_j$ across the elements. To further extend the definition, retarded partial coefficients of potential are defined that include the specification of the retardation time. Since the charges reside on the conductor surfaces, the potentials are only due to nodes external to the conductors. Therefore, generalized partial coefficients of potential can be written in matrix form as

$$\begin{bmatrix}\Phi_p{}^s\\ \hline \Phi_p{}^i\end{bmatrix} = \begin{bmatrix}pp^s\\ \hline pp^i\end{bmatrix}\boldsymbol{Q}_p \quad (18)$$

where Φ^i and pp^i correspond to the internal nodes, while $\Phi_p{}^s$, pp^s, and $\boldsymbol{Q}_p$ refer to the surface cells.

V. Retardation Time

The formulation given above is general in that it includes retardation times for widely spaced objects in a uniform dielectric region. As indicated in Sections III and VI, retarded partial inductances and retarded coefficients of potential can be defined for a network interpretation of the formulation. A basic difference between the wire antenna problem [16] and the interconnection systems considered here is that retardation times are large for the former, while for the latter they may be ignorably small. Furthermore, the coupling of minute signals from the antenna to the receiver is of interest. In contrast, for

circuit-type geometries only relatively strong intercoupling is of interest. This immediately suggests that sparsity can be introduced into the interactions by ignoring small coupling terms. For most situations, the small coupling elements are also the ones having larger retardation time.

VI. Circuit Interpretation

The surface portion of (18) can be interpreted in terms of multicapacitances for ignorably small retardation times. Coefficients of partial capacitance are defined elsewhere [7] as $cp = pp^{-1}$, which corresponds to a full network of capacitances for the partial surfaces. Partial capacitances that are obtained from exact computations [7]–[9] represent a local improvement over the uniformly charged cells assumed above. The second portion of (18) must be interpreted as a set of dependent charge-controlled potential sources for nodes inside the conductors. A differential relation can be obtained for these nodes from (17) as

$$\dot{v}_{+,-} = \sum_{k=1}^{K} \sum_{m=1}^{M_k} I_{mk}[pp_{i(mk)^+} - pp_{i(mk)^-}] \qquad (19)$$

where i represents all internal nodes and I is the *capacitive* node current. To summarize, the capacitive terms for the surface nodes are taken into account by a set of multicapacitances, while internal nodes are represented by charge-controlled voltage sources. An example is given in Fig. 3 for a complete equivalent circuit for a corner of the rectangular conductor shown in Figs. 1 and 2. The inductances in the equivalent circuit are simply the partial inductances [6] of the cells while the cell resistance computations are trivial. The equivalent circuit is entered into a general-purpose network analysis program [10]–[12] to obtain the responses of interest. This solution approach results in a very flexible computer tool. Essentially, three types of analysis are performed—capacitance, inductance, and network analysis. General formulations exist for all these tasks such that responses for a wide range of geometries can be computed.

VII. Approximations and Results

For circuit geometries of practical interest all conductors are assumed to be located on a set of parallel planes. Static Green functions are used to approximate the inclusion of layers with different dielectric constants. These Green functions are available from three-dimensional capacitance computation methods [7]–[9]. In fact, for most circuit-type geometries they are directly included in the capacitances computed. Close agreement has been obtained between a measurement and responses from a PEEC solution for loops located on a dielectric substrate for fast rising pulses with a spectrum into the gigahertz range [13].

An approximate description of the geometry often results in considerable savings in set-up and computation time. Responses for models of a different complexity are compared to find whether sufficiently small cells have been chosen. An example is again given in [13]. The change of L and R with frequency is less pronounced for conductors that are not closely spaced and that are not located near ground planes. Thus very often the conductors can be represented by a few nodes only. A typical example for rather large loops is given in Fig. 4. The responses of interest are found in the time domain rather than frequency domain using the ASTAP program [12]. The cross section of the conductors is 1.2 mm × 50 μm, while the horizontal geometry shown in Fig. 4 is located on a substrate with $\epsilon_r = 4$. A discussion is appropriate concerning the choice of the cells for the problem at hand. The long and thin conductors are not divided further in the cross-sectional dimensions. Partitions that delimit the inductance and capacitance cells are chosen at convenient

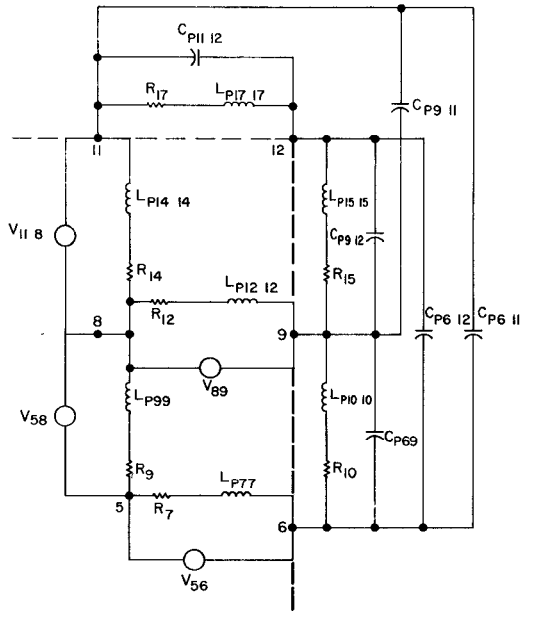

Fig. 3. Equivalent circuit for corner of a conductor.

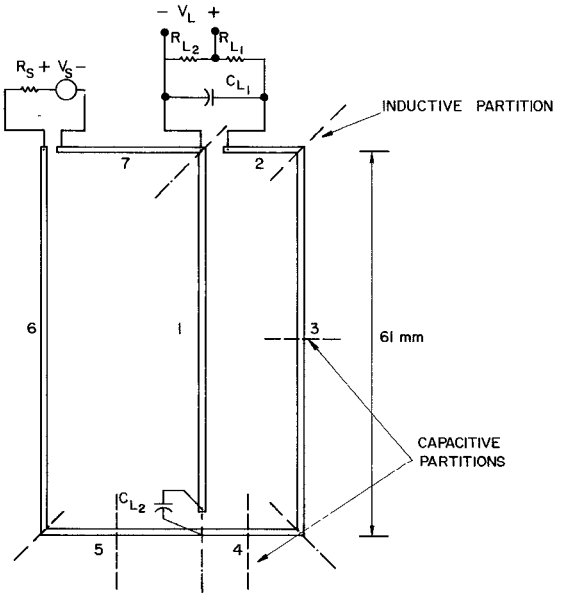

Fig. 4. Conductors on insulating substrate.

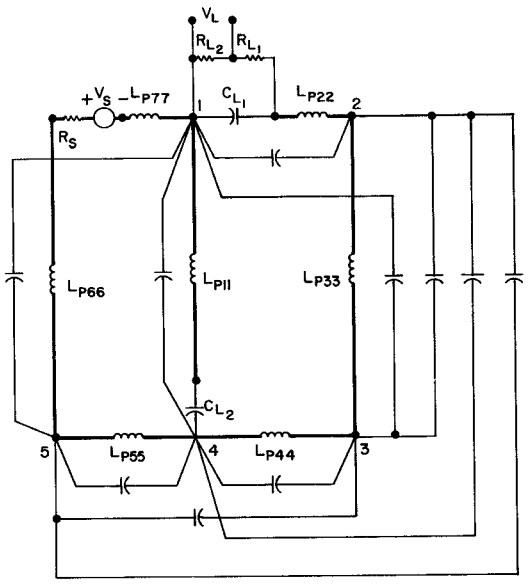

Fig. 5. Partial element equivalent circuit. Partial capacitances labeled according to node numbers.

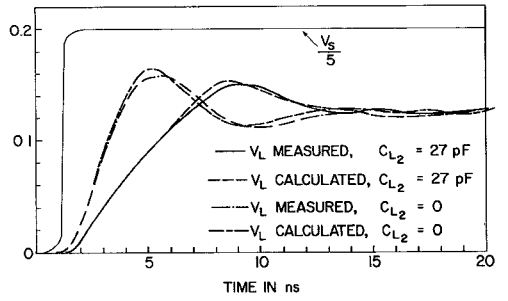

Fig. 6. Time domain response.

points along the length of the conductors as indicated in Fig. 4. The series resistance of the wires is ignored for this case and all retardation times are assumed to be 0. The source and loads can be arbitrary but an arrangement is chosen here that permits a measurement. The PEEC model shown in Fig. 5 is based on the relatively large cells chosen, yet they lead to a rather accurate representation of the time domain responses shown in Fig. 6 with only 17 circuit elements. The two responses shown are examples with or without C_{L2} connected. The partial capacitances C_{pij} [7] listed in Table I are in "node-pair form," a representation that is obtained by transforming all capacitances to the node at infinity in parallel to the node-pair capacitances. This is obtained by a generalized star–triangle transformation.

VIII. Conclusions

The PEEC models presented in this paper lead to a flexible solution technique both in the time domain and the frequency domain mainly due to the availability of computer formulations. Essentially, three computer analyses must be performed, viz., inductance computations, capacitance computation, and network analysis. The series resistance can usually be found from simple calculations. Changes in the geometry are easily accomodated since general computer solutions are involved in the task.

It is noted that the PEEC models are rather inefficient for two-dimensional geometries, especially if a high degree of resolution is required. For three-dimensional geometries, very good results are obtained with a few elements only, as is exemplified in Section VII.

TABLE I
List of Network Elements

$R_s = 50$	$L_{p55} = 21$	$C_{p12} = .61$
$R_{L1} = 300$	$L_{p66} = 59$	$C_{p13} = .525$
$R_{L2} = 50$	$L_{p77} = 20$	$C_{p14} = .225$
$C_{L1} = 8$	$L_{p13} = 14.7$	$C_{p15} = .725$
$C_{L2} = 27$	$L_{p16} = -10.6$	$C_{p23} = .285$
$L_{p11} = 57.2$	$L_{p27} = 2$	$C_{p25} = .275$
$L_{p22} = 10.2$	$L_{p36} = -7.7$	$C_{p34} = .125$
$L_{p33} = 62.1$	$L_{p45} = 2.4$	$C_{p35} = .275$
$L_{p44} = 11.6$	$L_{p57} = -1$	$C_{p45} = .225$
R in ohms; L in nH; C in pF		

Acknowledgment

The author wishes to thank M. Handelsman of the University of Vermont for many helpful discussions on the subject.

References

[1] A. E. Ruehli, "Electrical considerations in the computer-aided design of logic circuit interconnections," in *Proc. ACM-IEEE 10th Annu. Design Automation Workshop* (Portland, Oreg., June 1973).
[2] M. Caulton, B. Hershenov, S. P. Knight, and R. E. DeBrecht, "Status of lumped elements in microwave integrated circuits—Present and future," *IEEE Trans. Microwave Theory Tech. (Special Issue on Microwave Integrated Circuits)*, vol. MTT-19, pp. 588–599, July 1971.
[3] H. Amemiya, "Time-domain analysis of multiple parallel transmission lines," *RCA Rev.*, pp. 241–276, June 1967.
[4] C. W. Ho, "Theory and computer-aided analysis of multiple coupled transmission lines," in *Proc. IEEE Int. Symp. Circuit Theory* (North Hollywood, Calif., Apr. 1972), pp. 13–15.
[5] N. B. Rabbat, "Computer-aided transient response of multiple coupled unequal transmission lines," in *Proc. IEEE Int. Symp. Circuit Theory* (Toronto, Ont., Canada, Apr. 1973), pp. 217–219.
[6] A. E. Ruehli, "Inductance calculations in a complex integrated circuit environment," *IBM J. Res. Develop.*, vol. 16, pp. 470–481, Sept. 1972.
[7] A. E. Ruehli and P. A. Brennan, "Efficient capacitance calculations for three-dimensional multiconductor systems," *IEEE Trans. Microwave Theory Tech.*, vol. MTT-21, pp. 76–82, Feb. 1973.
[8] P. Silvester and P. Benedek, "Equivalent capacitances of microstrip open circuits," *IEEE Trans. Microwave Theory Tech.*, vol. MTT-20, pp. 511–516, Aug. 1972.
[9] P. D. Patel, "Calculation of capacitance coefficients for a system of irregular finite conductors on a dielectric sheet," *IEEE Trans. Microwave Theory Tech.*, vol. MTT-19, pp. 862–869, Nov. 1971.
[10] F. H. Branin, G. R. Hogsett, R. Lunde, and L. E. Kugel, "Ecap II–An electronic circuit analysis program," *IEEE Spectrum*, vol. 8, pp. 14–25, June 1971.
[11] W. T. Weeks, A. J. Jimenez, C. W. Mahoney, H. Qassemzadeh,

and T. R. Scott, "Network analysis using a sparse tableau with tree selection to increase sparseness," *in Proc. IEEE Int. Symp. Circuit Theory* (Toronto, Ont., Canada, Apr. 1973), pp. 165–168.
[12] *IBM Advanced Statistical Analysis Program*, ASTAP manual GH20-1271-0.
[13] A. E. Ruehli, "Electrical analysis of interconnections in a solid-state circuit environment," in *Dig. IEEE Int. Solid-State Circuit Conf.* (New York, 1972), pp. 64–65 and p. 216.
[14] E. C. Jordan and K. G. Balmain, *Electro-Magnetic Waves and Radiating Systems*. Englewood Cliffs, N. J.: Prentice-Hall, 1968, ch. 14.
[15] A. Gopinath and P. Silvester, "Calculation of inductance of finite-length strips and its variation with frequency," *IEEE Trans. Microwave Theory Tech.*, vol. MTT-21, pp. 380–386, June 1973.
[16] R. F. Harrington, *Field Computation by Moment Methods*. New York: Macmillan, 1968, ch. 1 and 4.

An Iterative Approach to the Finite-Element Method in Field Problems

W. KINSNER, MEMBER, IEEE, AND EDWARD DELLA TORRE, SENIOR MEMBER, IEEE

***Abstract*—An iterative approach to the finite-element method is presented. Several finite-element formulations are presented for the Laplace, Poisson, and Helmholtz equations. These formulations permit iterative solutions. The convergence of the vector sequences generated by the iterative method is accelerated using successive extrapolation and other methods. Accuracy and convergence of the solutions are discussed.**

I. Introduction

THE THEORETICAL background of the finite-element method has been given by Aubin [1]. Other authors [2], [3] have introduced some practical aspects of the method as applied to structural mechanics. Silvester [4] and others [5], [16], [20]–[22] discussed the method as applied to the electromagnetic field problems. Convergence of the method, as a function of the relative size of the discretizing elements and the order of the approximating polynomials, is discussed in many recent mathematical and technical journals [6]. In particular, explicit discretization errors are given in [1], [2], [6], and [7], and some experimental results are given in [5] and [8].

The variational formulation of waveguide problems, using complete polynomials, leads to the general eigenvalue problem

$$A\boldsymbol{x} = \lambda B\boldsymbol{x} \tag{1}$$

where A and B are symmetric positive-definite $n \times n$ band matrices, λ is the eigenvalue(s) and $\boldsymbol{x}$ the eigenvector(s) associated with the particular eigenvalue(s). It is noted that for the H modes A is only semidefinite. The finite-difference formulation of these problems also leads to (1), however, the matrix B is the identity matrix, and A is not necessarily symmetric.

A variety of methods for solving (1) have been presented (e.g., [9], [10], and [12]). The finite-difference solutions most frequently employ iterative techniques and the finite-element solutions almost exclusively use direct methods.

Iterative methods for solving eigenvalue problems may be divided into two categories. The first methods use the fact that eigenvectors of a system form a linearly independent set which spans an n dimensional space. The methods in the second category use the property that the generalized Rayleigh quotient

$$Q = \frac{\boldsymbol{x}^T A\boldsymbol{x}}{\boldsymbol{x}^T B\boldsymbol{x}} \tag{2}$$

is equal to an eigenvalue and is stationary when $\boldsymbol{x}$ is the corresponding eigenvector. A method using this property with Fletcher–Powell iteration has been described [13]. These methods combined with the deflation or orthogonalization yield, however, only partial eigensolutions, i.e., the dominant and several closest eigenvectors. An iterative method for the complete eigensolution shall be presented.

II. Finite-Element Formulation

Let R be either a simply or multiply-connected bounded region in an n dimensional space V^n with boundary Γ. The boundary Γ consists of a finite number of closed, nonintersecting hypersurfaces $\Gamma_h (h = 0, \cdots, \tau)$ such

Manuscript received June 26, 1973; revised November 7, 1973. This work was supported by the National Research Council of Canada.

The authors are with the Group on Simulation, Optimization, and Control, Department of Electrical Engineering, McMaster University, Hamilton, Ont., Canada.